Chemosphere 187 (2017) 294–301

Contents lists available at ScienceDirect

Chemosphere

journal homepage: www.elsevier.com/locate/chemosphere

Pb concentrations and isotopic record preserved in northwest Greenland snow

Jung-Ho Kang [a, *], Heejin Hwang [a], Changhee Han [a, b], Soon Do Hur [a], Seong-Joong Kim [c], Sungmin Hong [b, **]

[a] Division of Polar Paleoenvironment, Korea Polar Research Institute (KOPRI), 26 Songdomirae-ro, Incheon, 21990, Republic of Korea
[b] Department of Ocean Sciences, Inha University, Incheon, 22212, Republic of Korea
[c] Division of Polar Climate Sciences, Korea Polar Research Institute (KOPRI), 26 Songdomirae-ro, Incheon, 21990, Republic of Korea

HIGHLIGHTS

- Pb records investigated from a 3.2-m snow pit in northwest Greenland.
- Northwest Greenland snow is highly enriched with anthropogenic Pb.
- Pb concentrations exhibit seasonal peaks in winter–spring layers.
- $^{206}Pb/^{207}Pb$ ratios have gradually increased between 2003 and 2009.
- Contribution of Pb from China was very large through winter 2005–spring 2006.

GRAPHICAL ABSTRACT

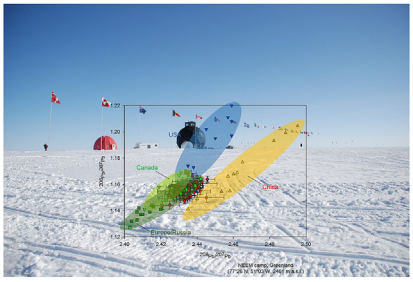

ARTICLE INFO

Article history:
Received 14 April 2017
Received in revised form
18 July 2017
Accepted 18 August 2017
Available online 30 August 2017

Handling editor: Martine Leermakers

Keywords:
Lead concentration
Lead isotope ratio
Enrichment factor
Greenland snow

ABSTRACT

We present high-resolution lead (Pb) concentrations and isotopic ratios from a northwest Greenland snow pit covering a six-year period between 2003 and 2009. Pb concentrations ranged widely from 2.7 pg g^{-1} to 97.3 pg g^{-1}, with a mean concentration of 21.6 pg g^{-1}. These values are higher than those recorded for the pre-industrial period. Pb concentrations exhibit seasonal spikes in winter–spring layers. Crustal Pb enrichment factors (EF) suggest that the northwest Greenland snow pit is highly enriched with Pb of predominantly anthropogenic origin. The $^{206}Pb/^{207}Pb$ ratios ranged from 1.144 to 1.169 with a mean value of 1.156, which fall between less radiogenic Eurasian-type and more radiogenic Canadian-type signatures. This result suggests that several potential source areas of Pb impact on northwest Greenland. Abrupt changes in Pb concentrations and Pb isotope ratios were observed and related to seasonal shifts in source regions of aerosol transport. The $^{206}Pb/^{207}Pb$ isotope ratio increased gradually between 2003 and 2009. The similarity of the three-isotope plot ($^{206}Pb/^{207}Pb$ versus $^{208}Pb/^{207}Pb$) between some of our samples and Chinese urban aerosols suggests a steadily increasing contribution of Chinese Pb to northwest Greenland snow.

1. Introduction

Lead (Pb) concentrations in the Greenland ice sheet have altered dramatically as a result of anthropogenic Pb, which is influenced by civilization, industrialization, and environmental policy. The first

* Corresponding author.
** Corresponding author. Department of Ocean Sciences, Inha University, Incheon, 22212, Republic of Korea.
E-mail addresses: jhkang@kopri.re.kr (J.-H. Kang), smhong@inha.ac.kr (S. Hong).

http://dx.doi.org/10.1016/j.chemosphere.2017.08.101
0045-6535/

record of Pb pollution in the Greenland ice sheet dates from 2500 years ago, during the peak period of Greco-Roman civilization (Hong et al., 1994). Hong et al. (1994) measured Pb concentrations in ice sections of the 3028 m GRIP ice core dated from 7760 years–470 years ago. Natural Pb concentrations in the Greenland ice sheet were about 0.5 pg g^{-1} between 7700 and 3000 years ago, increasing to 3 pg g^{-1} at the apogee of the Roman Empire (i.e., six times higher than natural values) owing to Pb and Ag production during the Greek and Roman periods. Pb concentrations declined to 0.7 pg g^{-1} around 1500 years ago with the fall of the Roman Empire, and then increased continuously during Medieval and Renaissance times.

Pb concentrations in the Greenland ice sheet continued to increase steadily from the 1750s (~10 pg g^{-1}) to the 1900s (~50 pg g^{-1}) as a consequence of anthropogenic Pb emissions mainly from nonferrous metal smelting production and coal combustion in the Northern Hemisphere (Murozumi et al., 1969). Starting from the 1930s, a rapid increase was then observed in Greenland snow and ice, reaching peak concentrations in the late 1960s (~200-fold above the natural values) (Murozumi et al., 1969; Candelone et al., 1995; McConnell and Edwards, 2008). This enormous increase was mainly linked to the very extensive use of Pb additives in gasoline from the early 1920s (Nriagu, 1990). Increased Pb pollution, as recorded from the Greenland ice sheet, contributed to a change in environmental perception and to the adoption of environmental policies; for example, the Clean Air Act of 1970, which sought to reduce air pollution in the United States, focusing on reduced use of leaded gasoline. Policies to phase out leaded gasoline have been effective in reducing atmospheric Pb concentrations, with evidence for this found in Greenland snow. Following the decline in use of leaded gasoline in the United States and other countries, Pb concentrations in the Greenland ice sheet dropped significantly from the late 1960s onward (Boutron et al., 1991).

Pb concentrations in the Greenland ice sheet remain high compared to those of the pre-industrial period (Barbante et al., 2003). From 1981 to 1990, Pb concentrations in snow from central Greenland varied widely, from 4.3 pg g^{-1} to 160 pg g^{-1} (Sherrell et al., 2000). Following the global phase out of leaded gasoline (i.e., since the 1980s), Asian industrial emissions of Pb from coal combustion and metal smelting have become the principal source of Pb in the North Pacific atmosphere (Osterberg et al., 2008). Asia has become the largest anthropogenic source of trace metals in the atmosphere and China-emitted aerosols account for a substantial and growing fraction of anthropogenic Pb deposited in Greenland (Bory et al., 2014); however it is still unclear how much of anthropogenic Pb is deposited in Greenland and there are limited data indicating recent variations in Pb concentrations in Greenland snow.

The four stable isotopes of Pb (^{204}Pb, ^{206}Pb, ^{207}Pb and ^{208}Pb) can act as a powerful geochemical tracer (Komárek et al., 2008). In snow and ice, Pb isotope ratios can be used not only to distinguish natural Pb from anthropogenic Pb, but also to identify specific potential source areas. The Pb isotopic composition of ores and industrial Pb varies globally but is regionally consistent. By comparing Pb isotope ratios in natural archives to those of regional emission sources, atmospheric transport pathways and mixing processes can be determined. For example, the isotope characteristics of a three-isotope plot (^{206}Pb/^{207}Pb versus ^{208}Pb/^{207}Pb) in Greenland ice samples identified the Southern Spanish mining region as the dominant sources of anthropogenic Pb emissions between 680 BCE and 193 AD (Rosman et al., 1997). Similarly, a steep increase in the ^{206}Pb/^{207}Pb isotope ratio of Greenland snow core sections indicates that the United States became a significant source between 1967 and 1975, with the subsequent decrease in the ^{206}Pb/^{207}Pb isotope ratio after 1976 attributed to lower but constant input of Pb from Eurasia and Canada (Rosman et al., 1993, 1994).

In this study, we investigated temporal profiles of Pb concentrations and isotopic ratios from a 3.2 m depth snow pit near the North Greenland Eemian Ice Drilling (NEEM) camp in northwest Greenland. We investigated Pb concentrations and isotopic ratios to expand our understanding of recent variations in Pb deposition and Pb sources.

2. Material and methods

2.1. Field sampling

As a part of the NEEM project, we excavated a 3.2-m depth snow pit on 26 June 2009 at the NEEM study site (77°26′N, 51°03′W, 2461 m a.s.l.) in northwestern Greenland (Kang et al., 2015). We dug a snow pit using metal shovels and then shaved away about 10 cm of snow from the wall of the pit using pre-cleaned low density polyethylene (LDPE) shovels. A continuous series of 70 snow samples were collected by horizontally pushing an acid-cleaned polytetrafluoroethylene (PTFE) tube and hammer. The snow samples were placed in acid-cleaned 1 L LDPE bottles. Precautions were taken in the field to minimize the possibility of snow contamination (Hong et al., 2000). All sample bottles were transported frozen from the NEEM camp to the laboratory at the Korea Polar Research Institute (KOPRI) and kept frozen at −20 °C until analysis.

2.2. Sample preparation and instrumental analysis

Since contamination significantly affects the measurement of trace elements and Pb isotopes, we prepared the samples in a class 10 laminar airflow clean bench within class 1000 clean room facilities at KOPRI, and followed executed clean protocols to prevent contamination (Kang et al., 2015). Samples were thawed and aliquoted into 15 mL LDPE bottles. Bottles were cleaned prior to use, following a rigorous acid rinsing procedure (Hong et al., 2000).

All aliquots for trace element analysis were acidified to 1% “Optima” grade nitric acid (HNO_3) (Fisher Scientific, Canada). Concentrations of Pb and other trace elements were determined using Inductively Coupled Plasma-Sector Field Mass Spectrometry (ICP-SFMS; Element2, Thermo Scientific, Germany) equipped with an Apex HF high efficiency sample inlet system (Apex HF, Elemental Scientific, USA). Analytical instrumentation and ultra clean working conditions are described in detail by Hong et al. (2009). Special attention was given to daily optimization of instrumental parameters in order to obtain high intensities and minimize possible interference. Detection limits, defined as three times the standard deviation of 10 measurements of the blank (1% “Optima” grade HNO_3 solution in sub-boiled water) were 0.09 and 0.24 pg g^{-1}, for Pb and Ba, respectively. Data quality was estimated by analyzing the SLRS-5 riverine water certified reference material (National Research Council, Canada).

Full analytical procedures for Pb isotopic measurement are described in Han et al. (2015). Briefly, an approximately 10 mL aliquot was weighed into a preconditioned Teflon vial (Savillex, USA) containing 10 μL HNO_3 (Fisher “Optima” ultrapure grade), 20 μL hydrofluoric acid (HF, Merck “Ultrapur” grade), and 4 μL dilute phosphoric acid (H_3PO_4) (Merck “Suprapur” grade; approximately 5 wt% solution). The mixture was evaporated to dryness at sub-boiling temperature in a class 10 clean hood. The evaporated residue was mixed with a droplet of silica-gel activator and then transferred onto a degassed zone-refined rhenium filament. A

droplet on the filament was dried by passing an electric current at 1 A, then slowly increased to 2.2 A until leaving a faint white deposit on the filament. Samples for Pb isotopic composition were analyzed using thermal ionization mass spectrometry (TIMS; Triton, Thermo Scientific, Germany) at KOPRI. All ion beams were measured with a secondary electron multiplier (SEM) operated in ion counting mode. Two procedure blanks and two or more reference material samples containing 50 pg of NIST SRM 981 were also analyzed, together with each batch of up to 21 samples. Mean procedure blank levels of Pb were 0.34 ± 0.24 pg, accounting for less than 10% for a few tens of picograms of Pb in analyzed snow samples with very low concentrations of Pb (Han et al., 2015). Regular measurement of the NIST SRM 981 showed that there was a bias of ~0.2% in ^{208}Pb isotope abundance. The bias introduced into the isotopic ratios by evaporation of the samples and other unknown factors was determined by repeated measurement of NIST SRM 981 (Fig. S1; Table S1).

2.3. Dating of the snow pit

Dating of the snow pit was based on multiple parameters, including stable water isotopes ($\delta^{18}O$ and δD), and anion and cation measurements (Na^+, Ca^{2+}, Cl^-, SO_4^{2-}, and methanesulfonic acid (MSA)) (Kang et al., 2015). We defined maximum peaks of $\delta^{18}O$ and δD as summer and the minima as winter. Concentrations of Na^+, Cl^-, nss-Ca^{2+}, and nss-SO_4^{2-} in the snow pit indicated seasonal deposition events with maxima in winter–spring layers. Summer layers were characterized by maximum concentrations of MSA and the Cl^-/Na^+ ratio. Based on multiple dating parameters, the 3.2 m-depth snow pit was shown to cover a continuous period of six years of snow deposition, from spring 2003 to early summer 2009 (Kang et al., 2015).

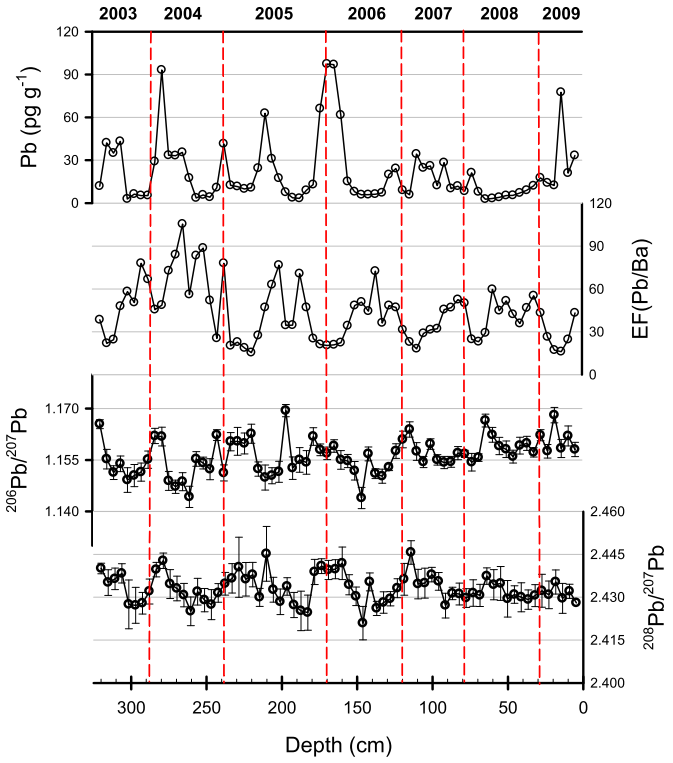

Fig. 1. Temporal profiles of Pb concentrations, Pb isotopes, and crustal enrichment factors (EF) in northwest Greenland snow (dashed red lines represent winter layers). (For interpretation of the references to colour in this figure legend, the reader is referred to the web version of this article.)

3. Results and discussion

3.1. Pb concentrations and seasonal variations

The depth profile of Pb concentrations is shown in Fig. 1. Pb concentrations varied widely, from 2.7 pg g^{-1} to 97.3 pg g^{-1}, with a mean concentration of 21.6 pg g^{-1} (Table 1). High Pb concentrations (>25 pg g^{-1}) were prominent, with seasonal peaks in winter–spring layers (before and after the $\delta^{18}O$ minimum). The highest Pb concentration was recorded from the winter 2005–spring 2006 layers. This Pb peak is clearly associated with a dust episode well marked in the same snow layer (Kang et al., 2015). On the other hand, anomalous high Pb concentration peaks were also observed within layers corresponding to late spring–summer 2005 and late spring 2009. Interestingly, Pb concentrations for the whole of 2008 were at a low level and showed no distinct seasonality.

Seasonal variations in Pb concentrations have been reported in previous studies, notably during winter–spring seasons. A decade-long (1981–1990) seasonal record of Pb concentrations from a central Greenland snow pit (ATM site) showed seasonal variability, with maxima in spring layers (Sherrell et al., 2000). Similarly, a 2-year Pb record (1990–1992) from a central Greenland snow pit (ATM site) was characterized by high Pb concentrations in spring–summer layers (Candelone et al., 1996). In the southern Greenland ice sheet (Dye 3), high Pb concentrations occurred in spring layers, together with Cd, Cu, and Zn concentrations (Savarino et al., 1994). Such a comparison should be made with caution, taking into account the different latitudes, altitudes, and snow accumulation rates of the sites (NEEM, ATM, and Dye 3). There are no large spatial variations in seasonality along the latitudinal transect of the Greenland ice sheet.

The seasonality of the Pb input over the Greenland ice sheet is influenced by the Arctic climate system. Arctic Oscillations are known to be important in the delivery of contaminants to the Arctic environment (Macdonald et al., 2005). The maximum Pb input can be related to the seasonality of the North Atlantic Oscillation (or Artic Oscillation), which is connected with low pressure over Iceland and high pressure over Greenland. As the polar front extends across mid-latitude areas in winter, it can load and disperse large amounts of aerosols containing anthropogenic pollutants to polar areas through long-range atmospheric transportation (Savarino et al., 1994). The measurement of aerosol optical depth (AOD) and equivalent black carbon (EBC) during the period 2001–2011 could explain the maximum peak recorded in northern Greenland from late winter through spring in response to incursions of aerosols from lower latitudes (Stone et al., 2014). In addition, the high Pb concentrations occasionally occurring within layers other than winter–spring are associated with large precipitation events occurring at times of year when there is input of air masses containing anthropogenic pollutants. As transitions in atmospheric transport processes occurred during the period of analysis, abrupt seasonal changes in mineral dust particles deposited onto the NEEM site were observed (Kang et al., 2015).

3.2. Pb enrichment factors

The depth profiles of the Pb enrichment factors (EF) are shown in Fig. 1. We calculated the EF in order to estimate the nature of the Pb reaching the Greenland ice sheet (Burn-Nunes et al., 2014; Bazzano et al., 2016). The EF was defined as the concentration ratio of a given element to that of a conservative crustal element, normalized to the same concentration ratio characteristic of upper continental crust (Wedepohl, 1995). For example, in the case of barium (Ba), the calculation of the EF is as follows:

Table 1
Pb concentrations, Pb isotope compositions, and crustal enrichment factors in northwest Greenland snow.

Depth[a] (cm)	Pb (pg g^{-1})	±U[b]	$^{206}Pb/^{207}Pb$	±U[b]	$^{208}Pb/^{207}Pb$	±U[b]	$^{206}Pb/^{204}Pb$	±U[b]	Ba (pg g^{-1})	± U[b]	crustal EF[c]
5	33.3	0.40	1.158	0.002	2.428	0.003	17.862	0.098	30.2	1.67	43.3
9	21.0	0.39	1.162	0.003	2.432	0.002	18.008	0.083	33.5	1.70	24.6
14	77.5	3.23	1.158	0.003	2.430	0.005	17.864	0.080	189.3	10.02	16.1
18	12.3	0.07	1.168	0.002	2.435	0.004	18.086	0.085	28.2	0.88	17.2
23	14.1	0.26	1.158	0.002	2.431	0.005	17.915	0.081	21.0	0.92	26.3
27	17.7	0.21	1.162	0.002	2.432	0.006	18.009	0.086	16.1	1.03	43.2
32	12.1	0.10	1.157	0.001	2.431	0.004	17.949	0.077	8.6	0.11	55.2
37	8.9	0.11	1.160	0.002	2.429	0.003	17.904	0.070	7.5	0.16	46.8
41	7.0	0.37	1.159	0.002	2.430	0.005	17.977	0.098	7.7	0.81	35.9
46	5.3	0.20	1.156	0.002	2.431	0.003	17.878	0.093	5.0	0.13	42.2
50	5.2	0.06	1.158	0.002	2.429	0.006	17.890	0.185	4.0	0.32	51.6
55	4.0	0.15	1.159	0.003	2.435	0.006	17.927	0.180	3.5	0.41	44.8
59	3.1	0.07	1.162	0.002	2.434	0.005	17.970	0.112	2.1	0.03	59.7
64	2.7	0.13	1.166	0.002	2.437	0.003	17.986	0.116	3.6	0.03	29.2
69	7.8	0.07	1.156	0.001	2.431	0.004	17.911	0.116	13.4	0.20	23.0
73	21.2	0.29	1.154	0.003	2.431	0.005	17.868	0.142	33.8	0.81	24.7
78	8.2	0.22	1.157	0.001	2.430	0.003	17.887	0.119	6.4	0.21	50.0
82	11.8	0.15	1.157	0.002	2.431	0.004	17.901	0.065	8.8	0.19	52.6
87	10.1	0.07	1.154	0.002	2.431	0.002	17.811	0.093	8.5	0.54	46.9
91	28.2	0.45	1.154	0.002	2.427	0.004	17.842	0.102	24.4	0.66	45.5
96	12.2	0.28	1.155	0.002	2.436	0.003	17.853	0.073	15.0	0.94	32.1
101	26.0	0.34	1.160	0.002	2.438	0.003	17.896	0.063	32.5	1.85	31.4
105	24.6	0.33	1.154	0.002	2.435	0.005	17.861	0.052	33.5	2.97	28.9
110	34.3	0.41	1.157	0.003	2.435	0.005	17.943	0.182	74.4	2.79	18.1
114	5.8	0.13	1.164	0.002	2.446	0.004	18.053	0.102	10.0	0.87	22.9
119	8.9	0.04	1.161	0.002	2.436	0.006	18.030	0.052	11.2	0.41	31.4
123	24.1	0.35	1.158	0.002	2.433	0.003	17.895	0.089	20.2	0.33	47.1
128	19.9	0.17	1.153	0.001	2.429	0.003	17.805	0.059	16.2	0.63	48.4
133	7.1	0.07	1.150	0.002	2.428	0.004	17.795	0.090	7.7	1.07	36.2
137	6.1	0.05	1.151	0.001	2.426	0.002	17.811	0.066	3.3	0.11	72.4
142	5.9	0.11	1.157	0.002	2.435	0.003	17.883	0.097	5.2	0.73	44.5
146	5.8	0.05	1.144	0.003	2.421	0.006	17.544	0.161	4.5	0.22	50.8
151	7.9	0.12	1.152	0.003	2.430	0.003	17.811	0.092	6.4	0.20	48.3
155	15.1	0.21	1.155	0.002	2.434	0.004	17.856	0.117	17.4	1.86	34.2
160	61.6	0.92	1.155	0.003	2.442	0.006	17.821	0.121	108.0	9.17	22.4
165	96.9	1.03	1.159	0.002	2.440	0.003	17.884	0.070	182.6	4.78	20.9
169	97.3	0.91	1.159	0.002	2.440	0.003	17.884	0.070	187.2	5.29	20.4
174	66.1	0.51	1.158	0.002	2.441	0.003	17.887	0.073	122.9	2.86	21.1
178	12.9	0.30	1.162	0.003	2.439	0.004	17.969	0.083	20.2	0.43	25.2
183	8.9	0.06	1.154	0.003	2.425	0.006	17.528	0.164	7.4	0.18	47.1
187	3.2	0.04	1.155	0.004	2.425	0.007	17.848	0.170	1.8	0.01	70.7
192	3.7	0.06	1.153	0.003	2.427	0.004	17.893	0.095	4.2	0.07	34.6
197	7.5	0.06	1.169	0.002	2.434	0.003	18.065	0.070	8.6	0.26	34.5
201	17.4	0.37	1.152	0.003	2.428	0.004	17.819	0.143	8.9	0.16	76.7
206	30.9	0.24	1.150	0.002	2.433	0.004	17.646	0.121	19.3	0.83	62.9
210	62.8	0.70	1.150	0.004	2.445	0.010	17.728	0.192	52.6	1.04	46.9
215	24.3	0.34	1.152	0.002	2.430	0.003	17.757	0.075	34.9	1.02	27.4
219	10.7	0.19	1.163	0.003	2.438	0.004	18.003	0.090	27.1	1.46	15.5
224	9.9	0.10	1.160	0.003	2.436	0.006	17.900	0.142	20.9	0.74	18.7
229	11.5	0.11	1.160	0.004	2.441	0.011	18.079	0.174	19.9	0.75	22.8
233	12.4	0.12	1.160	0.003	2.437	0.005	18.005	0.089	24.1	0.11	20.2
238	41.5	0.23	1.151	0.002	2.435	0.004	17.797	0.074	20.9	0.62	78.0
242	10.8	0.28	1.162	0.002	2.432	0.003	17.991	0.108	16.6	0.28	25.5
247	4.1	0.03	1.152	0.003	2.427	0.005	17.905	0.143	3.1	0.05	51.9
251	5.6	0.04	1.154	0.002	2.429	0.004	17.914	0.139	2.5	0.11	88.6
256	3.5	0.03	1.155	0.002	2.432	0.005	17.882	0.125	1.6	0.06	83.3
260	17.5	0.13	1.144	0.003	2.425	0.005	17.731	0.119	12.3	0.36	56.1
265	35.5	0.73	1.149	0.003	2.431	0.004	17.757	0.105	13.2	0.28	105.4
270	33.2	1.05	1.147	0.002	2.433	0.004	17.716	0.086	15.5	0.25	84.0
274	33.4	1.33	1.149	0.003	2.435	0.005	17.745	0.122	18.0	0.29	72.6
279	93.2	0.60	1.162	0.003	2.443	0.003	17.939	0.126	75.2	3.29	48.7
283	29.0	0.51	1.162	0.002	2.440	0.003	18.034	0.098	25.1	1.18	45.5
288	5.2	0.05	1.155	0.003	2.432	0.004	17.865	0.088	3.0	0.16	66.7
292	5.2	0.04	1.151	0.003	2.428	0.004	17.826	0.053	2.6	0.07	78.0
297	6.2	0.05	1.150	0.003	2.427	0.006	17.792	0.157	4.8	0.09	50.5
302	2.8	0.04	1.149	0.004	2.428	0.009	17.878	0.108	1.9	0.08	58.1
306	43.2	0.73	1.154	0.002	2.438	0.003	17.808	0.118	35.5	0.28	47.8
311	35.0	1.47	1.151	0.002	2.436	0.004	17.778	0.209	56.0	0.92	24.5
315	42.1	0.24	1.155	0.003	2.435	0.005	17.820	0.141	75.6	2.14	21.9
320	11.8	0.32	1.165	0.001	2.440	0.002	18.073	0.043	12.1	0.15	38.5

[a] 0 cm corresponds to the surface in June 2009. Depth of 27, 78, 119, 169, 238, and 283 cm corresponds to the year of 2009, 2008, 2007, 2006, 2005, and 2004, respectively.
[b] Uncertainties are 95% confidence intervals.
[c] Crustal enrichment factors for Pb, calculated with Ba as a crustal reference metal (see text).

$$EF(Pb/Ba) = (Pb/Ba)_{snow}/(Pb/Ba)_{UCC}$$

where $(Pb/Ba)_{UCC}$ is the mean ratio for the upper continental crust (2.545×10^{-2}, according to Wedepohl, 1995). Recently, Ba has been used as a crustal reference element in many studies of Pb contamination in snow and ice. As a proxy for soil dust deposition, Ba concentrations are similar to Pb concentrations (Vallelonga et al., 2002; Burn-Nunes et al., 2014). EF(Pb/Ba) values ranged from 15.5 to 105.4, with a mean of 43.4 (Table 1). High values of EF(Pb/Ba) suggest that the snow pit samples are highly enriched with Pb, indicating a predominantly anthropogenic origin of atmospheric particulates other than natural origin of crustal dust particulates. The Pb enrichment factors in Greenland ice cores were ~1 at 3000 years ago and ~5 in the late 15th century (Hong et al., 1994). McConnell et al. (2002) reported Pb enrichment factors of ~30 prior to 1870, increasing to > 500 by 1970, and dropping to ~100 by 1985 (McConnell et al., 2002).

EF(Pb/Ba) values tend to be inversely correlated with Pb concentrations (Spearman coefficient; $r = -0.292$, $p < 0.05$). Much higher EF(Pb/Ba) values (>50) are observed when Pb concentrations are relatively lower, indicating the incursion of air masses incorporating with anthropogenic pollutants. On the other hand, lower EF(Pb/Ba) values (<30) are found with anomalous Pb peaks during winter 2005–spring 2006. This suggest a greater proportion of natural dust contributions from crustal sources. The enriched Pb frequently appears with crustal dust aerosol due to mixing of dust with anthropogenic pollutants on the transport pathways of air masses over long distances. In our samples, Pb concentrations are highly correlated with Ba concentrations ($r > 0.795$, $p < 0.01$). Pb concentrations also coincide with higher concentrations of non-sea-salt SO_4^{2-} ($r = 0.718$, $p < 0.01$), supporting co-occurrence of anthropogenic and crustal Pb (Kang et al., 2015). Therefore, it appears that the large fraction of Pb exceeding the crustal dust contribution in our samples is due to significant industrial Pb being supplied to Greenland (Barbante et al., 2003).

3.3. Pb isotopic compositions

The depth profile of the $^{206}Pb/^{207}Pb$ and $^{208}Pb/^{207}Pb$ ratios is shown in Fig. 1. The $^{206}Pb/^{207}Pb$ and $^{208}Pb/^{207}Pb$ ratios ranged from 1.144 to 1.169 with a mean value of 1.156 and from 2.421 to 2.446 with a mean value of 2.433, respectively (Table 1). Our $^{206}Pb/^{207}Pb$ ratios fall between less radiogenic Eurasian-type (~1.14) and more radiogenic Canadian-type (~1.17) signatures, suggesting several potential source areas of Pb reaching the northwest Greenland ice sheet (Rosman et al., 1994). An abnormally high value of the $^{206}Pb/^{207}Pb$ ratio was observed in the layer corresponding to the summer of 2005 ($^{206}Pb/^{207}Pb = 1.169$); however, the high radiogenic Mississippi Valley-type (>1.20) signatures were not found in any snow pit samples, indicating that high radiogenic Pb additives of leaded gasoline from United States sources did not contribute to the Pb deposited in northwest Greenland during the study period. Unusually high radiogenic Mississippi Valley-type Pb isotope ratios were imprinted on the central Greenland ice sheet until 1993, despite of the phase-out of leaded gasoline in the United States (Bory et al., 2014). High radiogenic Pb was emitted from smelters in the United States in the mid-1990s (Graney and Landis, 2013), but the $^{206}Pb/^{207}Pb$ ratio, ranging from 1.169 to 1.240, in precipitation samples across the Great Lakes region between 2003 and 2007 supported that the high radiogenic Pb contribution from the United States has been decreasing (Sherman et al., 2015).

The $^{206}Pb/^{207}Pb$ and $^{208}Pb/^{207}Pb$ ratios display seasonal variations with more radiogenic signal in winter–spring layers and less radiogenic signal in summer–fall layers (Fig. 1). Distinct seasonal variations were recorded in fresh snow samples collected at Dye 3 in Southern Greenland (Rosman et al., 1998). From 1988 to 1989, the $^{206}Pb/^{207}Pb$ ratio was ~1.14 in spring–summer snow, reaching ~1.20 in winter snow. These large differences in $^{206}Pb/^{207}Pb$ ratios indicate that aerosols falling onto the Greenland ice sheet originate from various directions, including the Canadian Arctic, Northern America, the North Atlantic, and Asia, depending on season and transitions in atmospheric transport processes (Kang et al., 2015). Seasonal variability in the $^{206}Pb/^{207}Pb$ and $^{208}Pb/^{207}Pb$ ratio observed in our study indicates changes in the major sources of anthropogenic Pb inputs to northwest Greenland. Temporal changes in Pb isotope ratios can be related to seasonal shifts in source regions for the aerosols reaching the Greenland ice sheets.

3.4. Potential sources of anthropogenic Pb in northwest Greenland

Fig. 2 shows the isotopic characteristics of a three-isotope plot ($^{206}Pb/^{207}Pb$ versus $^{208}Pb/^{207}Pb$) of NEEM snow pit samples and aerosol particles from the Northern Hemisphere after the mid-1990s global phase out of leaded gasoline. We compared the isotopic data of the NEEM snow pit samples covering the period between 2003 and 2009 with those of aerosol particles from the Northern Hemisphere. Urban aerosols collected from Europe, Russia, Canada, and East Asia showed the geographical variations in the Pb isotopic composition (Bollhöfer and Rosman, 2001). In addition to tracing potential source areas for anthropogenic Pb, Pb isotopic compositions can also provide information about the mixing history of air masses (Rosman et al., 1998). As shown in Fig. 2, isotopic compositions in the NEEM snow pit are scattered along a narrow range of values, rather than along the mixing line. The Pb isotopic composition of Northern Hemisphere urban aerosols allows definition of broad continental trends, even if global industrial sources make it difficult to use Pb isotopic fingerprinting following the phase out of leaded gasoline (Bory et al., 2014). Data from Mongolia was spread out over the NEEM range, suggesting that some of the Pb deposited in Greenland during the period studied might also be derived from Asia. Indeed, recent modeling of global dust emissions and transport clearly support the view that central Asia is a significant source of aerosols to Greenland (Uno et al., 2009). It is apparent that the Pb isotopic composition of some NEEM samples show a trend that moves toward the direction of the distinct Chinese isotopic domain (Ewing et al., 2010; Bory et al., 2014). Data from Chinese urban cities, loess fractions, and coals form a linear array that is shifted toward higher values of $^{208}Pb/^{207}Pb$ (Jones et al., 2000; Bollhöfer and Rosman, 2001; Díaz-Somoano et al., 2009; Ewing et al., 2010). Chinese urban aerosols stand out as a distinctive end-member, with higher $^{208}Pb/^{207}Pb$ for a given $^{206}Pb/^{207}Pb$ ratio (Bory et al., 2014).

According to the estimation of Bory et al. (2014), the relative influence of Chinese anthropogenic sources increased during spring season and a large fraction (up to >50%) of the insoluble Pb deposited in central Greenland was sourced to China during the spring of 2001 (Bory et al., 2014). We have estimated the relative weight of the Chinese contribution based on the similar calculations used by Ewing et al. (2010) and Bory et al. (2014) as below,

$$\Delta^{208}Pb_{observed} = [^{208}Pb/^{207}Pb_{observed} - {}^{208}Pb/^{207}Pb_{baseline}]_{206}$$

$$\Delta^{208}Pb_{China} = [^{208}Pb/^{207}Pb_{observed} - {}^{208}Pb/^{207}Pb_{China}]_{206}$$

$$F_{China\ (208Pb/207Pb)}\ (\%) = \Delta^{208}Pb_{observed}/\Delta^{208}Pb_{China} \times 100$$

where $^{208}Pb/^{207}Pb_{baseline}$ is derived from the regression line of Greenland snow (Rosman et al., 1994) and $^{208}Pb/^{207}Pb_{China}$ is derived from the regression line of the distinct Chinese isotopic

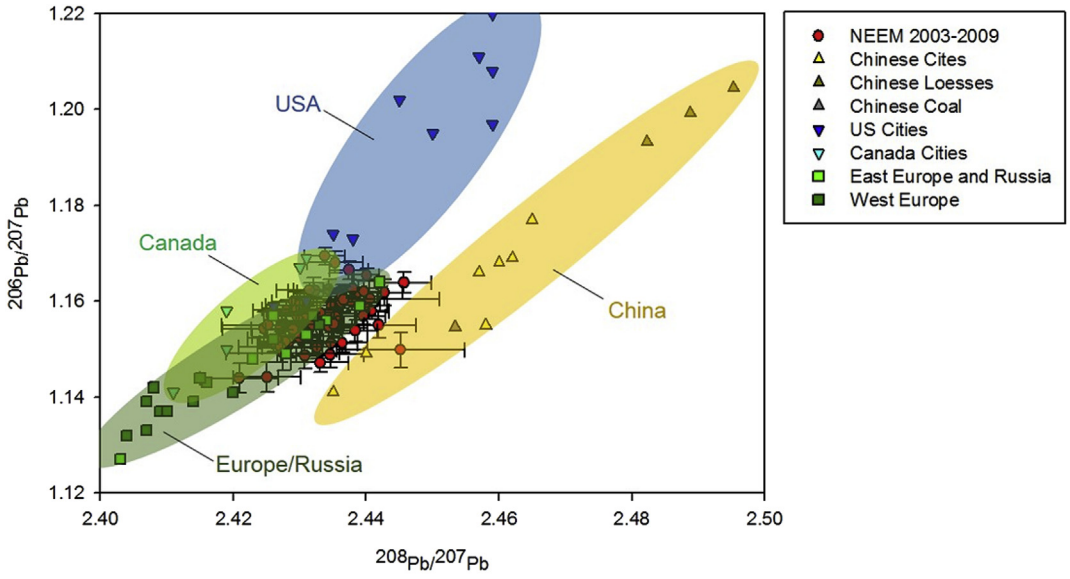

Fig. 2. $^{206}Pb/^{207}Pb$ versus $^{208}Pb/^{207}Pb$ for the NEEM snowpit and aerosol particles from Northern Hemisphere cities (Bollhöfer and Rosman, 2001; Ewing et al., 2010), Chinese coal (Díaz-Somoano et al., 2009), and Chinese loesses (Jones et al., 2000).

domain in Fig. S3. Positive $\Delta^{208}Pb$ and $\Delta^{206}Pb$ indicate contribution from Chinese sources. Using the estimation, Chinese source is attributed to up to 73% of the Pb in the NEEM samples during the period in winter 2005–spring 2006. The regression line of isotope ratios in the NEEM snow pit shifted toward the distinctive Chinese urban aerosols end-member. This is consistent with observations of Asian aerosol *trans*-Pacific transport to western North America (Osterberg et al., 2008; Ewing et al., 2010). The proportion of Asian Pb was up to 80%–93% in Mt. Tamalpais and in central California cities, which was elevated through the springtime period (Ewing et al., 2010).

3.5. Dynamic time series of Pb concentrations and Pb isotopes in Greenland ice sheets

Time series Pb concentrations are plotted in Fig. 3(a). Table 2 summarizes Pb concentrations from recently-dug snow pits in Greenland, together with those of a snow pit in Devon Island, Canadian Arctic. To the best of our knowledge, our data represent the most recent Pb records deposited into the northwest Greenland ice sheet. By the end of the 1960s, Pb concentrations increased steeply to 318 pg g^{-1}, before falling by one order of magnitude by 1995 (Barbante et al., 2003). Our Pb concentrations are lower than the highest Pb concentrations from the 1960s–1970s. As noted above, following the phase out of leaded gasoline in the United States and other countries, atmospheric Pb emissions and deposition onto the Greenland ice sheet decreased dramatically; however, despite such a drop in Pb concentrations during the 1980s–1990s, they did not return to pre-industrial levels (Candelone et al., 1996; Sherrell et al., 2000; Barbante et al., 2003). Pb concentrations in Greenland snow from 1981 to 1990 were observed to be within the range of 3.0–158 pg g^{-1} (Savarino et al., 1994; Sherrell et al., 2000). Candelone et al. (1996) recorded a similar data range (0.6–44 pg g^{-1}) from a 1.6 m-depth snow pit in central Greenland covering the period 1990–1992. Pb concentrations in central Greenland ranged from 2.0108 pg g^{-1}, with a mean concentration of 17.3 pg g^{-1}, in the period 1991–1995 (Barbante et al., 2003). In comparison, mean Pb concentrations in the period 2003–2005 were statistically different and slightly higher than in 1991–1995 (when two outlier samples are omitted; $p < 0.05$). Owing to limited data from the Greenland snow pit and from the period 1995–2000s, this increase in Pb concentrations requires further investigation. It is also of note that, outside Greenland, analysis of snow precipitation on Devon Island (Canadian Arctic) indicated a predominance of industrial Pb in recent snow (1994–2004), with a mean of 45.2 pg g^{-1} (Shotyk et al., 2005). Pb concentrations in northwest Greenland snow seem to be increasing because of the rapid growth of (and consequent increase in Pb emissions from) Asian industries (McConnell and Edwards, 2008; Osterberg et al., 2008).

Time series Pb isotopes are plotted in Fig. 3(b). As noted before, temporal changes in Pb isotope ratios were used to identify the provenance of Pb (Rosman et al., 1993, 1994, 1997, 1998). The long-term trend of the isotope ratio suggests a shift in potential Pb sources. The $^{206}Pb/^{207}Pb$ ratio increased after the 1960s, reaching its maximum value by about 1976, before decreasing back to the initial ratio by the 1980s (Rosman et al., 1994). The increase after the 1960s was due to an increasing proportion of highly radiogenic Mississippi Valley-type Pb in leaded gasoline. The decrease after 1976 was attributed to the reduction in the consumption of leaded gasoline in the United States and other countries. The time trend of the $^{206}Pb/^{207}Pb$ ratio of our samples (red circles) seems to have increased steadily between 2003 and 2009, indicating continuous input of more radiogenic Pb particulates, with mixed provenance from several Pb source regions. Isotopic compositions were similar to the isotope ratios from the Devon Island snow pit, ranging between 1.131 and 1.170; in the case of Devon Island, these are likewise influenced by dominant industrial sources of atmospheric Pb (Shotyk et al., 2005). The $^{206}Pb/^{207}Pb$ ratios of our samples are within similar ranges of the $^{206}Pb/^{207}Pb$ isotope ratio of Chinese urban aerosols, remaining approximately constant at 1.160 (Cheng and Hu, 2010).

4. Conclusions

Our study outlines high-resolution Pb concentrations and Pb isotopes from a northwest Greenland snow pit covering a six-year period between 2003 and 2009. Despite a rapid decline in Pb concentrations since the phase out of leaded gasoline, Pb concentrations remain higher than those of the pre-industrial period and

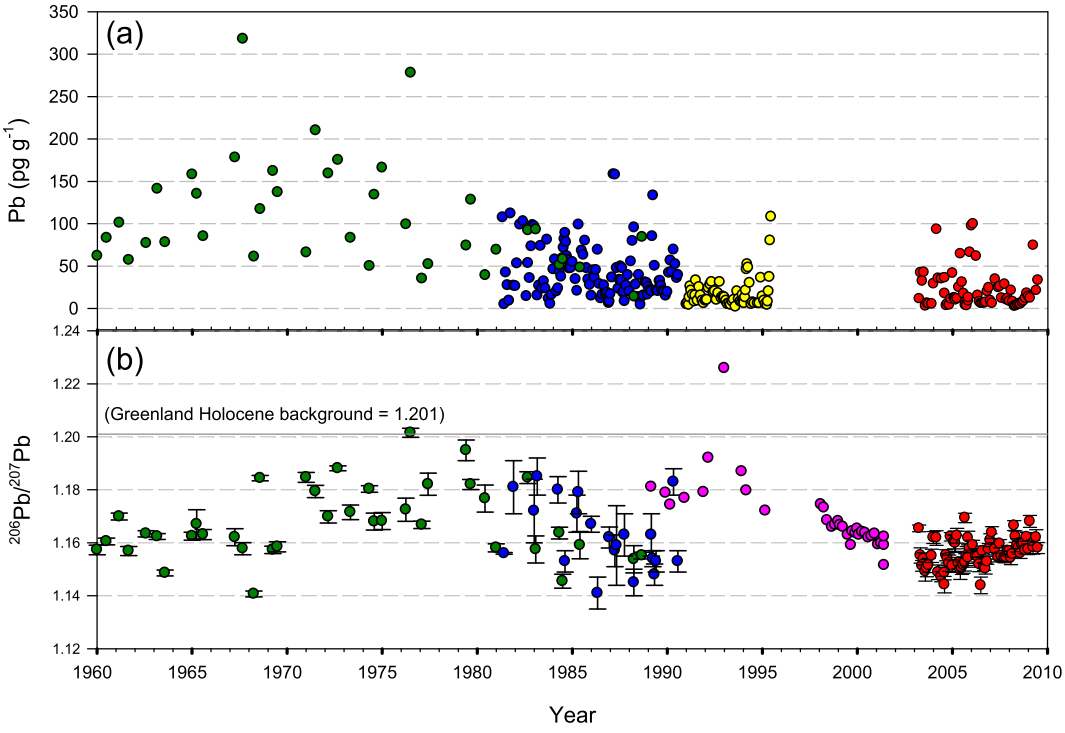

Fig. 3. Comparison of Pb concentrations (a) and Pb isotope ratios (b) from the Greenland Ice Sheet (NEEM snow pit; red circles), summit snow pit (yellow circles, Barbante et al., 2003), ATM snow pit (blue circles, Sherrell et al., 2000), summit snow core (green circles, Rosman et al., 1994), and NGRIP insoluble particles (purple circles, Bory et al., 2014) as well as Greenland Holocene (preindustrial) background (gray solid line at ^{206}Pb/^{207}Pb = 1.201, Rosman et al., 1997). (For interpretation of the references to colour in this figure legend, the reader is referred to the web version of this article.)

Table 2
Comparison of Pb concentrations (pg g^{-1}) from recently-dug snow pits in Greenland with those from a snow pit in Devon Island, Canadian Arctic.

	Location	Analytical method	Time Period	Average Pb Conc.	Range
This work (2017)	NEEM	ICP-SFMS	2003–2009	21.6	2.7–97.3
Shotyk et al. (2005)	Devon	ICP-SFMS	1994–2004	45.2	1.0–165
Barbante et al. (2003)	Summit	ICP-SFMS	1991–1995	17.3	2.0–108
Candelone et al. (1996)	ATM	GFAAS	1990–1992	15	0.6–44
Savarino et al. (1994)	GISP2	GFAAS	1989–1990	18	2.5–47
Sherrell et al. (2000)	ATM	GFAAS	1981–1990	43.6	4.3–160

show a steady increase in concentration during the period investigated. The ^{206}Pb/^{207}Pb and ^{208}Pb/^{207}Pb ratios display higher radiogenic values and Pb concentrations in winter–spring snow, and lower radiogenic values and Pb concentrations from summer to autumn. The isotopic data indicate that the Pb reaching northwest Greenland originates from several potential source areas, with an increasing contribution from coal consumption in China. A fraction of the Chinese Pb contribution estimated by the isotopic composition (Δ^{208}Pb and Δ^{206}Pb) is observed to increase particularly between winter 2005 and spring 2006.

Acknowledgments

This work was supported by a research grant (PE17040) from the Korea Polar Research Institute (KOPRI). We are thankful for the efforts of all field personnel involved in sampling during the NEEM deep ice core drilling project. The NEEM project was directed and organized by the Center for Ice and Climate at the Niels Bohr Institute and the Polar Programs Office of the US National Science Foundation. The project was supported by funding agencies and institutions in Belgium (FNRS-CFB and FWO), Canada (NRCan/GSC), China (CAS), Denmark (FIST), France (IPEV, CNRS/INSU, CEA and ANR), Germany (AWI), Iceland (Rannls), Japan (NIPR), Korea (KOPRI), Netherlands (NOW/ALW), Sweden (VR), Switzerland (SNF), the UK (NERC), and the USA (US NSF OPP).

Appendix A. Supplementary data

Supplementary data related to this article can be found at http://dx.doi.org/10.1016/j.chemosphere.2017.08.101.

References

Barbante, C., Boutron, C., Morel, C., Ferrari, C., Jaffrezo, J.L., Cozzi, G., Gaspari, V., Cescon, P., 2003. Seasonal variations of heavy metals in central Greenland snow deposited from 1991 to 1995. J. Environ. Monit. 5, 328–335.
Bazzano, A., Cappelletti, D., Udisti, R., Grotti, M., 2016. Long-range transport of atmospheric lead reaching Ny-Ålesund: inter-annual and seasonal variations of potential source areas. Atmos. Environ. 139, 11–19.
Bollhöfer, A., Rosman, K.J.R., 2001. Isotopic source signatures for atmospheric lead: the Northern Hemisphere. Geochimica Cosmochimica Acta 65, 1727–1740.
Bory, A.J.M., Abouchami, W., Galer, S.J.G., Svensson, A., Christensen, J.N., Biscaye, P.E., 2014. A Chinese imprint in insoluble pollutants recently deposited in Central Greenland as indicated by lead isotopes. Environ. Sci. Technol. 48, 1451–1457.
Boutron, C.F., Gorlach, U., Candelone, J.-P., Bolshov, M.A., Delmas, R.J., 1991. Decrease in anthropogenic lead, cadmium and zinc in Greenland snows since the late 1960s. Nature 353, 153–156.
Burn-Nunes, L., Vallelonga, P., Lee, K., Hong, S., Burton, G., Hou, S., Moy, A.,

Edwards, R., Loss, R., Rosman, K., 2014. Seasonal variations in the sources of natural and anthropogenic lead deposited at the East Rongbuk Glacier in the high-altitude Himalayas. Sci. Total Environ. 487, 407–419.
Candelone, J.P., Hong, S., Pellone, C., Boutron, C.F., 1995. Post-Industrial Revolution changes in large-scale atmospheric pollution of the northern hemisphere by heavy metals as documented in central Greenland snow and ice. J. Geophys. Res. Atmos. 100, 16605–16616.
Candelone, J.P., Jaffrezo, J.L., Hong, S., Davidson, C.I., Boutron, C.F., 1996. Seasonal variations in heavy metals concentrations in present day Greenland snow. Sci. Total Environ. 193, 101–110.
Cheng, H., Hu, Y., 2010. Lead (Pb) isotopic fingerprinting and its applications in lead pollution studies in China: a review. Environ. Pollut. 158, 1134–1146.
Díaz-Somoano, M., Kylander, M.E., López-Antón, M.A., Suárez-Ruiz, I., Martínez-Tarazona, M.R., Ferrat, M., Kober, B., Weiss, D.J., 2009. Stable lead isotope compositions in selected coals from around the world and implications for present day aerosol source tracing. Environ. Sci. Technol. 43, 1078–1085.
Ewing, S.A., Christensen, J.N., Brown, S.T., Vancuren, R.A., Cliff, S.S., Depaolo, D.J., 2010. Pb isotopes as an indicator of the Asian contribution to particulate air pollution in urban California. Environ. Sci. Technol. 44, 8911–8916.
Graney, J.R., Landis, M.S., 2013. Coupling meteorology, metal concentrations, and Pb isotopes for source attribution in archived precipitation samples. Sci. Total Environ. 448, 141–150.
Han, C., Burn-Nunes, L.J., Lee, K., Chang, C., Kang, J.-H., Han, Y., Hur, S.D., Hong, S., 2015. Determination of lead isotopes in a new Greenland deep ice core at the sub-picogram per gram level by thermal ionization mass spectrometry using an improved decontamination method. Talanta 140, 20–28.
Hong, S., Candelone, J.P., Patterson, C.C., Boutron, C.F., 1994. Greenland ice evidence of hemispheric lead pollution two millennia ago by Greek and Roman civilizations. Science 265, 1841–1843.
Hong, S., Lee, K., Hou, S., Soon, D.H., Ren, J., Burn, L.J., Rosman, K.J.R., Barbante, C., Boutron, C.F., 2009. An 800-year record of atmospheric As, Mo, Sn, and Sb in central Asia in high-altitude ice cores from Mt. Qomolangma (Everest), Himalayas. Environ. Sci. Technol. 43, 8060–8065.
Hong, S., Lluberas, A., Rodriguez, F., 2000. A clean protocol for determining ultralow heavy metal concentrations: its application to the analysis of Pb, Cd, Cu, Zn and Mn in Antarctic snow. Korean J. Polar Res. 11, 35–47.
Jones, C.E., Halliday, A.N., Rea, D.K., Owen, R.M., 2000. Eolian inputs of lead to the North Pacific. Geochimica Cosmochimica Acta 64, 1405–1416.
Kang, J.-H., Hwang, H., Hong, S.B., Hur, S.D., Choi, S.-D., Lee, J., Hong, S., 2015. Mineral dust and major ion concentrations in snowpit samples from the NEEM site, Greenland. Atmos. Environ. 120, 137–143.
Komárek, M., Ettler, V., Chrastný, V., Mihaljevic, M., 2008. Lead isotopes in environmental sciences: a review. Environ. Int. 34, 562–577.
Macdonald, R.W., Harner, T., Fyfe, J., 2005. Recent climate change in the Arctic and its impact on contaminant pathways and interpretation of temporal trend data. Sci. Total Environ. 342, 5–86.
McConnell, J.R., Edwards, R., 2008. Coal burning leaves toxic heavy metal legacy in the Arctic. Proc. Natl. Acad. Sci. U. S. A. 105, 12140–12144.
McConnell, J.R., Lamorey, G.W., Hutterli, M.A., 2002. A 250-year high-resolution record of Pb flux and crustal enrichment in central Greenland. Geophys. Res. Lett. 29, 2130. http://dx.doi.org/10.1029/2002GL016016.
Murozumi, M., Chow, T.J., Patterson, C., 1969. Chemical concentrations of pollutant lead aerosols, terrestrial dusts and sea salts in Greenland and Antarctic snow strata. Geochimica Cosmochimica Acta 33, 1247–1294.
Nriagu, J.O., 1990. The rise and fall of leaded gasoline. Sci. Total Environ. 92, 13–28.
Osterberg, E.C., Mayewski, P., Kreutz, K., Fisher, D., Handley, M., Sneed, S., Zdanowicz, C., Zheng, J., Demuth, M., Waskiewicz, M., Bourgeois, J., 2008. Ice core record of rising lead pollution in the North Pacific atmosphere. Geophys. Res. Lett. 35, L05810. http://dx.doi.org/10.01029/02007GL032680.
Rosman, K.J.R., Chisholm, W., Boutron, C.F., Candelone, J.P., Gorlach, U., 1993. Isotopic evidence for the source of lead in Greenland snows since the late 1960s. Nature 362, 333–335.
Rosman, K.J.R., Chisholm, W., Boutron, C.F., Candelone, J.P., Hong, S., 1994. Isotopic evidence to account for changes in the concentration of lead in Greenland snow between 1960 and 1988. Geochimica Cosmochimica Acta 58, 3265–3269.
Rosman, K.J.R., Chisholm, W., Boutron, C.F., Candelone, J.P., Jaffrezo, J.L., Davidson, C.I., 1998. Seasonal variations in the origin of lead in snow at Dye 3, Greenland. Earth Planet. Sci. Lett. 160, 383–389.
Rosman, K.J.R., Chisholm, W., Hong, S., Candelone, J.P., Boutron, C.F., 1997. Lead from Carthaginian and Roman Spanish mines isotopically identified in Greenland ice dated from 600 B.C. to 300 A.D. Environ. Sci. Technol. 31, 3413–3416.
Savarino, J., Boutron, C.F., Jaffrezo, J.L., 1994. Short-term variations of Pb, Cd, Zn and Cu in recent Greenland snow. Atmos. Environ. 28, 1731–1737.
Sherman, L.S., Blum, J.D., Dvonch, J.T., Gratz, L.E., Landis, M.S., 2015. The use of Pb, Sr, and Hg isotopes in Great Lakes precipitation as a tool for pollution source attribution. Sci. Total Environ. 502, 362–374.
Sherrell, R.M., Boyle, E.A., Falkner, K.K., Harris, N.R., 2000. Temporal variability of Cd, Pb, and Pb isotope deposition in central Greenland snow. Geochem. Geophys. Geosys. 1, 1002. http://dx.doi.org/10.1029/1999GC000007.
Shotyk, W., Zheng, J., Krachler, M., Zdanowicz, C., Koerner, R., Fisher, D., 2005. Predominance of industrial Pb in recent snow (1994–2004) and ice (1842–1996) from Devon Island, Arctic Canada. Geophys. Res. Lett. 32, L21814. http://dx.doi.org/10.21029/22005GL023860.
Stone, R., Sharma, S., Herber, A., Eleftheriadis, K., Nelson, D., 2014. A characterization of Arctic aerosols on the basis of aerosol optical depth and black carbon measurements. Elem. Sci. Anth 2. http://dx.doi.org/10.12952/journal.elementa.000027.
Uno, I., Eguchi, K., Yumimoto, K., Takemura, T., Shimizu, A., Uematsu, M., Liu, Z., Wang, Z., Hara, Y., Sugimoto, N., 2009. Asian dust transported one full circuit around the globe. Nat. Geosci. 2, 557–560.
Vallelonga, P., Van de Velde, K., Candelone, J.P., Morgan, V.I., Boutron, C.F., Rosman, K.J.R., 2002. The lead pollution history of Law Dome, Antarctica, from isotopic measurements on ice cores: 1500 AD to 1989 AD. Earth Planet. Sci. Lett. 204, 291–306.
Wedepohl, K.H., 1995. The composition of the continental crust. Geochimica Cosmochimica Acta 59, 1217–1232.